Solar Energy Materials & Solar Cells 285 (2025) 113493

Contents lists available at ScienceDirect

Solar Energy Materials and Solar Cells

journal homepage: www.elsevier.com/locate/solmat

Evaluation of parameters to characterize the aging of solar reflector materials

Johannes Wette [a,*], Florian Sutter [b], Ricardo Sánchez-Moreno [a], Florian Wiesinger [b], Aránzazu Fernández-García [a]

[a] Centro de Investigaciones Energéticas, Medioambientales y Tecnológicas (CIEMAT), Plataforma Solar de Almería (PSA), Ctra. de Senés/n km 4, Apartado 22, 04200, Tabernas, Spain

[b] German Aerospace Center (DLR), Institute of Solar Research, Calle Doctor Carracido Nr. 44, 1st floor, 04005, Almería, Spain

ARTICLE INFO

Keywords:
Concentrating solar thermal technology
Solar reflector material
Degradation parameter
Long duration accelerated aging
Corrosion
Reflectance

ABSTRACT

The evaluation of the degradation of solar reflectors for concentrating solar thermal applications is of primary importance for material development and to guarantee the optimal optical quality of the solar field over an extended life time. Standardization of durability tests and their evaluation is very limited nowadays and an important ongoing task contributing to the reliability and feasibility of the technology. In this work, a series of long duration accelerated aging tests were used to test a set of different reflector materials, from commercial to experimental and low-cost materials, and by taking the durations to extreme levels never before conducted, assuring the appearance of considerable degradation. The most common degradation parameters were determined and a thorough evaluation of the tests, the parameters and their determination techniques was performed. The copper-accelerated acetic acid salt spray test was confirmed to be the quickest test to provoke degradation in most materials and this way offers the possibility to compare different candidates. Other tests provoke little degradation for most materials even after long durations. The development of corrosion spots is the first parameter to show differences for the materials. The specular reflectance is more sensitive to show degradation than the hemispherical reflecance. An overview table was created which allows to determine minimum test durations to select, depending on the parameter and test to be evaluated. This serves as an important tool for the planning of future tests and may help with the further standardization of testing and evaluation of the durability of solar reflectors.

Nomenclature

Symbols	
d_{corr}	Corrosion spot density [1/cm^2]
RH	Relative humidity [%]
T	Temperature [°C]
θ_i	Incidence angle [°]
λ	Wavelength [nm]
ρ	Reflectance [−]
$\rho_{\lambda,h}$	Spectral near-normal hemispherical reflectance [−]
$\rho_{s,h}$	Solar-weighted near-normal hemispherical reflectance [−]
$\rho_{s,\varphi}$	Solar-weighted near-normal near-specular reflectance [−]
$\rho_{\lambda,\varphi}$	Spectral near-normal near-specular reflectance [−]
$\Delta\rho$	Reflectance difference (after testing minus initial) [−]
φ	Acceptance (half) angle [mrad]

(*continued on next column*)

(*continued*)

Acronyms	
CASS	Copper-accelerated acetic acid salt spray test
COND	Condensation test
CST	Concentrating solar thermal
CIEMAT	*Centro de Investigaciones Energéticas, Medioambientales y Tecnológicas*
DH	Damp heat test
DLR	*Deutsches Zentrum für Luft- und Raumfahrt*
D&S	Devices & Services
NSS	Neutral salt spray test
OPAC	Optical Aging Characterization Laboratory
PSA	Plataforma Solar de Almería
PV	Photovoltaic
TCH	Thermal cycling and humidity test
UV	Ultraviolet
UVH	UV/humidity test

* Corresponding author.
E-mail addresses: johannes.wette@web.de, johannes.wette@psa.es (J. Wette).

https://doi.org/10.1016/j.solmat.2025.113493
Received 29 November 2024; Received in revised form 31 January 2025; Accepted 6 February 2025
Available online 14 February 2025

1. Introduction

For many years, concentrating solar thermal (CST) technologies have been recognized as one of the key technologies to tackle the decarbonization of the world's energy system by replacing fossil energy sources with renewable ones [1,2]. Even though the worldwide installed capacity of CST is small compared to other technologies as solar photovoltaics (PV) and wind power, the potential for its future growth is mainly seen in its capacity for the implementation of low cost, efficient energy storage and the direct supply of process heat [1,3,4]. One of the key challenges to be addressed for enabling the continuous success of the technology is to drive down costs of the overall systems. One of the main cost factors of all CST systems is their solar field. The solar field, usually comprising parabolic-trough concentrators or heliostats, is responsible for the concentration of the incoming direct solar irradiation onto a receiver. The quality of the mirrors used in the solar fields plays a crucial role in determining the optical efficiency of the system [5]. Two of the required key characteristics of the solar mirrors are high reflectance and high durability to maintain initial properties over the lifetime of the systems. Assuring these characteristics is important to guarantee the long term maximum optical yield of the CST plants and thus helps to prove their viability. The vast majority of CST projects uses silvered-glass mirrors as the reflector material [6], due to its favorable features and long track record for the use in the technology [7]. Other materials have been investigated for many years and are being used for special, less widespread designs [8–10], but due to their low market share, the focus of this work is on the silvered-glass mirrors as the effective industry standard.

Durability testing of solar mirrors is usually a combination of long term outdoor exposure and accelerated aging in the laboratory [11]. The outdoor exposure is used to identify degradation mechanisms appearing under realistic in-service conditions and the accelerated testing intends to reproduce these mechanisms in a shorter time frame, avoiding unrealistic side effects which are not created under outdoor conditions. Once suitable tests and conditions are established, these can be used to assess the durability of new materials in a relatively quick and reliable manner. The most common applications are the development of lifetime prediction procedures [12] or simple material comparisons and pass/fail tests [13]. The first standard specifically published on the accelerated aging of the solar mirrors was and is up until today the Spanish national standard UNE 206016–2018 [14]. The IEC technical committee TC 117 - subcommittee PT 62862-3-6 is working on the development of the first international standard on the topic, which is expected to be published during 2025 under the title "Durability of silvered-glass reflectors - Laboratory test methods and assessment". Standardization of the accelerated aging procedures is an important step, which allows different parties to reach comparable results and increase reproducibility of the results by fulfilling the requirements and keeping parameter limits established in these standards.

The tests used for accelerated laboratory testing are mostly adopted from other more mature industry sectors, as for example the automotive industry. Duration and parameters of the tests have to be adapted for the specific requirements for solar mirrors. The tests usually consist of the placement of mirror samples in chambers, exposing them to conditions in which one or several environmental parameters are increased compared to outdoor conditions [15]. The appropriate selection of the parameters is crucial to reach a reasonable acceleration of the degradation without provoking unrealistic side effects due to too extreme conditions. The two main categories of tests are climate chamber tests provoking a chemical attack and mechanical tests. The climate chamber tests work with parameters such as increased temperature, humidity and radiation as well as the possible addition of chemical agents such as salt, chlorides or corrosive gases, while the mechanical tests simulate the direct impact of effects such as erosion by airborne sand particles [16] or mechanical cleaning with brushes [17,18]. This publication addresses the chemical degradation, considering the respective climate chamber tests.

The UNE 206016-2018 standard [14] comprises five climate chamber tests: two direct corrosion tests, neutral salt spray (NSS) and copper accelerated salt spray (CASS); and three tests with elevated temperature and humidity, including one under constant conditions (typically known as condensation, COND), one with cyclic conditions (named as thermal cycling and humidity, TCH), and a last one with the addition of ultraviolet (UV) radiation (named as UV/Humidity, UVH). An additional common test for reflectors, that was introduced for concentrator PV cells [19] and is included in the planned IEC standard, consists of exposure to constant high temperature and humidity (typically known as damp heat, DH). Further, less well established tests combining different sets of parameters, are being conducted throughout industry and academia [20–23]. The duration of the tests depends on their aggressiveness and usually ranges from 120 h for the most aggressive tests up to around 2000 h for the more innocuous ones, without specifying the amount of degradation this provokes. Previous studies have shown that marginal degradation is expected for state-of-the-art materials after these standard durations [24]. Manufacturers of solar mirrors usually publish information on results of a selection of these standard tests at not-well established durations with pass/fail criteria [25], without giving details on the measured degradation parameters.

For the evaluation of mirror samples and their degradation, a wide range of parameters is available. First of all, standards for testing usually require to record any changes of the materials detected, without regard of their nature. More specifically, a set of parameters has been defined describing certain kinds of degradation mechanisms and effects to be able to monitor and evaluate the most common appearing defects in solar mirrors. The main parameter determining the quality of solar mirrors, i.e. their ability to reflect and redirect the solar radiation, is the reflectance, ρ. A range of different reflectance parameters exist which mainly differ in the incidence angle, ϑ_i, the acceptance angle, φ, and the wavelength of the radiation, λ. The most meaningful parameter really determining the reflectance for CST applications is the solar-weighted near-normal near-specular reflectance, $\rho_{s,\varphi}$ [26–28]. This parameter is difficult to measure and only few experimental measurement setups are available in specialized labs to determine it [29–31]. Due to the lack of an appropriate commercial measurement system, other reflectance parameters are used which are easier to determine. The two most common ones are the solar-weighted near-normal hemispherical reflectance, $\rho_{s,h}$, and the monochromatic near-normal near-specular reflectance, $\rho_{\lambda,\varphi}$, which can be measured with commercial spectrophotometers and reflectometers, respectively. Another shortcoming of reflectance measurements is that they are performed on certain spots without covering larger areas. Ideally, the mean reflectance of the whole mirror surface would be determined. In practice, a series of punctual measurements are taken and the average value is calculated.

In addition, further parameters are determined that indirectly influence the mirror reflectance, mainly by reducing the reflective area. For that, the corroded area is determined optically, counting the number of corrosion spots appearing in the silver layer, as well as measuring the penetration of corrosion of the silver layer starting at the edges of the samples. Microscopic imaging is recommended to monitor and analyze details of the defects in the reflective layer. Manual counting is still the standard procedure for the determination of the corrosion spot density, while automatic image analysis is more suitable for high numbers of spots, as recommended in the IEC PT 62862-3-6 draft, together with determination of the affected area, as proposed in Ref. [32].

Added parameters are described that have no direct influence on the optical quality but can be an indicator of future degradation of the reflective layer. These are especially changes of the back paint systems used to protect the reflective layer, covering damages like scratches and blistering or color changes such as yellowing [22,33].

Identification of these degradation parameters and the

determination of suitable ones, which may depend on the application and the material type, is the crucial first step for the evaluation of the tests and the further use of the results. For pass/fail tests suitable criteria and limits have to be considered as shown in Ref. [13]. For the use in lifetime prediction, it has to be assured that the parameter's development correlates with outdoor testing under realistic conditions. In Ref. [34] an advanced cyclic test was conducted on several materials and results were compared to outdoor behavior. In the conclusions it is stressed that test and parameter selection is crucial for the evaluation of the different materials, together with the deeper understanding of the degradation mechanisms. Different PV materials were tested in Ref. [35] in a combined cyclic test and it was found that correlations and their quality depend on material and parameter (optical, chemical, thermo-mechanical). Correlations were determined between color change of the back paint of silvered-glass mirrors and reflectance in high temperature tests in Ref. [36]. By modelling these correlations, it was possible to predict outdoor behavior of the materials. In Ref. [37] mass loss and optical imaging was used to compare material behavior in two accelerated tests [20]. presents the evaluation of extensive historical data to find correlations between accelerated and outdoor behavior of a variety of materials based on different reflectance parameters. A lifetime prediction model is developed in Ref. [12] by taking into account the combined effect of different mechanisms (erosion, corrosion, etc.) in different accelerated tests and comparing it to outdoor behavior. A comprehensive overview of modelling approaches for lifetime prediction is presented in Ref. [38] together with prerequisites for the execution of campaigns to determine these models and the model parameters.

The focus of this research work is the evaluation of the degradation parameters used for the analysis of solar mirror materials, specifically the three most common parameters included in the standards: reflectance, corrosion spots and edge corrosion penetration. The determination techniques as well as the reached magnitudes of the standard degradation parameters are thoroughly discussed from a scientific point of view for the first time. As a reliable way to achieve the required degradation for detection and to show differences between materials, the standard laboratory tests are conducted with an extended duration on a variety of different commercial as well as novel silvered-glass reflector types. The duration of the tests is strongly extended, from the traditionally conducted of 120–2000 h to 6000 h, a duration never reached on this kind of material up until now, to assure the presence of considerable representative degradation. This substantial degradation permits to provide indications on the appropriateness of the durations and the assessing parameters proposed in the available standards and manufacturer datasheets.

2. Methods and materials

This section introduces the six accelerated aging tests included in the study, the seven different silvered-glass reflector materials that were tested and the degradation parameters assessed, which are typically determined on a regular basis. The whole study presented in this publication was carried out by the OPAC (Optical Aging Characterization Laboratory) group, a permanent collaboration between the CIEMAT (*Centro de Investigaciones Energéticas, Medioambientales y Tecnológicas*) Materials for CST Technologies Unit and the DLR (*Deutsches Zentrum für Luft-und Raumfahrt*) Institute of Solar Research, at the CIEMAT-Plataforma Solar de Almería (PSA).

2.1. Durability tests

Six standardized accelerated aging tests, the five from the UNE 206016 standard [14] and the DH test [19], were performed for this study. The description of the tests is collected in Table 1, where T is the temperature and RH is the relative humidity in the chamber. The duration of the tests was increased to extreme levels of 6000 h for all the tests, except for the CASS test, which was stopped after 2280 h (or less for materials of lower durability) due to the strong degradation suffered by many of the materials. The TCH test was performed for 70 cycles, a long extension compared to the 10 cycles proposed in the standard. One cycle lasts roughly 24 h, depending on the cooling and heating ramps of the respective chambers, which are not completely fixed in the standard parameters. With that, the 70 cycles correspond to roughly 1680 h. To assure acceptable reproducibility of the results, the environmental parameters and testing conditions defined in the respective standards were controlled throughout the execution of all tests. Due to the known sensitivity of corrosion tests applying salt spray [39,40], to the testing conditions, the corrosivity in the chambers is regularly checked with standard metal coupons. For this, standardized steel coupons are tested with the other materials and it is checked that their mass loss due to corrosion is within the limits defined in [41].

Table 1
Conducted accelerated aging tests with used chamber models, minimum and actual duration, and testing conditions.

Test	Chamber model (manufacturer)	Minimum duration in UNE 206016 standard	Duration in this study	Summary of testing conditions
Neutral Salt Spray (NSS)	Corrosion chamber 608 (Erichsen)	480 h	6000 h	$T = 35 \pm 2$ °C, pH: 6.5 to 7.2 at 25 °C; NaCl solution 50 ± 5 g/l; condensation rate of 1.5 ± 0.5 ml/h on 80 cm^2 surface
Copper-accelerated acetic acid salt spray (CASS)	Salt spray chamber VSC450 (Vötsch)	120 h	2280 h	$T = 50 \pm 2$ °C, pH: 3.1 to 3.3 at 25 °C; NaCl solution 50 ± 5 g/l and 0.26 ± 0.02 g/l $CuCl_2$; Condensation rate 1.5 ± 0.5 ml/h on 80 cm^2 surface
Condensation (COND)	Climatic Chamber CKEST-300 (Ineltec)	480 h	6000 h	$T = 40 \pm 3$ °C; $RH = 100$ %
Combined thermal cycling and humidity (TCH)	Climatic Chamber SC340MH (Vötsch)	10 cycles	70 cycles	1 cycle: 4 h at $T = 85$ °C, 4 h at $T = -40$ °C, 16 h at T = 40 °C and $RH = 97 \pm 3$ %
UV/Humidity (UVH)	UVTest chamber (ATLAS)	2000 h	6000 h	4 h UV exposure at $T = 60 \pm 3$ °C followed by 4 h at $RH = 100$ % at $T = 50 \pm 3$ °C
Damp Heat (DH)	Test chamber HCP108 (Erichsen)	2000 h[a]	6000 h	$T = 65 \pm 2$ °C; $RH = 85 \pm 5$ %

[a] Duration proposed in the IEC 62108 standard for PV panels [19] and in actual draft version of the IEC 62862-3-6 draft standard for solar reflectors.

2.2. Materials

Seven materials were selected for testing, all of them silvered-glass mirrors, delivered by two different manufacturers (here called A and B for confidentiality concerns). Both manufacturers have a long track record of developing and producing solar mirrors for CST systems and have supplied mirrors for major commercial CST projects. The main characteristics of the materials are presented in Table 2. These materials were provided during the EU Horizon 2020 RAISELIFE project [42] and,

Table 2
Tested silvered-glass reflector materials of the two manufacturers with main characteristics.

Material	Manufacturer	Characteristics
RLA1	A	Commercial 3-layer paint system
RLA1R	A	As 1 but reduced paint thickness
RLA3	A	Experimental lead-free 2-layer system
RLA4	A	Experimental low cost 2-layer system
RLA4R	A	As 4 but reduced paint thickness
RLB1	B	Commercial 2-layer paint system
RLB3	B	Experimental low-cost 2-layer system

consequently, in the codification used, the first two letters (RL) correspond to the name of the project. The numbers in the material code refer to different used protective back-side paint systems (1, 3, 4 for manufacturer A and 1, 2 for B) and the letter R in two material codes indicates, that the applied layer thickness is lower than for the standard material without the R. These two materials were especially manufactured for the durability tests during the RAISELIFE project to possess lower durability and yield faster results by increased degradation. Both 1-materials (RLA1 and RLB1) represent the commercial product of the respective manufacturer and the others are experimental materials for research purposes. For the experimental materials, the number of paint layers as well as their chemical composition was modified by the manufacturer. Details of the composition of the used protective layer systems cannot be given due to confidentiality reasons and are only of secondary importance, because in this study the focus is laid on the influence of the duration in the test results and evaluation parameters. The materials were prepared in the industrial coating lines of the manufacturers as real size flat facets and then cut to samples of 10×10 cm^2 size for testing. All samples contain at least one original edge finish, the rest are cut-edges. Three samples were used per material and test to account for possible material heterogeneities and all values for the measurement parameters are the average of all three samples of the same type. For future studies focused on other specific materials (e.g. other manufacturers, curved trough or coated reflectors), it is recommended to repeat the tests with the respective specific material sample.

2.3. Parameters and measurements

In this section, the three degradation parameters used for the evaluation are presented, and their determination techniques are described.

2.3.1. Reflectance

Reflectance measurements were performed according to the newest version of the "SolarPACES Reflectance Guideline" [43]. To determine the $\rho_{s,h}$, the spectral near-normal hemispherical reflectance, $\rho_{\lambda,h}$, was measured with a PerkinElmer (PE) Lambda 1050 spectrophotometer. $\rho_{\lambda,h}$ measurements were performed in λ = [320, 2500] nm, using 5 nm intervals at $\vartheta_i = 8°$, with an integrating sphere of 150 mm diameter. The data was evaluated with a 2nd surface reference reflectance standard (calibrated in the range from 300 to 2500 nm), traceable to NIST. Three measurements were taken on each sample, in different spots. Following ASTM Standard E903-82 (92) [44], $\rho_{s,h}$ was calculated by weighting $\rho_{\lambda,h}$ with the solar direct irradiance G_b on the earth surface for each λ. For European and North American latitudes, typical solar irradiance spectra are given by the current standard ASTM G173-03 [45] (direct irradiance) for air mass AM 1.5. Uncertainties for these measurements were reported to be 0.008 [46].

The $\rho_{\lambda,\varphi}$, within a defined acceptance half-angle of $\varphi = 12.5$ mrad, was measured with a Devices & Services (D&S) 15R-USB portable specular reflectometer. This instrument uses a parallel beam with an incidence angle of $\vartheta_i = 15°$ and a λ range between 635 and 685 nm, with a peak at $\lambda = 660$ nm. The uncertainty of the measurements with the D&S were determined to be 0.003 [46]. Due to the typically higher heterogeneity of the specular reflectance values, each sample was measured in five different positions, instead of three.

When possible, measurements were taken on the reflective surface on areas which were apparently unaffected by degradation. This could not be assured in cases of minimal unaffected areas available or very high density of corrosion spots. The average values of all three samples per material were calculated. To show the effect of the tests on the materials the differences in reflectance between before and after testing are presented. Monochromatic specular and solar hemispherical reflectance losses, $\Delta\rho_{\lambda,\varphi}$ and $\Delta\rho_{s,h}$, are calculated by subtracting the respective initial values from the values after testing. This way negative values correspond to reflectance losses.

2.3.2. Corrosion spots

The corrosion spot density, d_{corr}, is determined by counting the spots with naked eye on the samples or on photographic images taken of the sample surface, in cases of higher spot densities. As indicated in UNE 206016, usually, spots of a minimum diameter of around 200 μm are counted, as smaller spots are barely visible. In cases of diameters close to 200 μm, the size of the defects was checked with microscope images. The microscope used for imaging was a Zeiss Axio CSM700 with objectives of 10-50× magnification, depending on the case. For very high densities of corrosion spots, a maximum value of 1/cm^2, equivalent to 100 spots on the 10×10 cm^2 samples, was set as the upper limit, due to difficulties determining higher densities without automatic image acquisition. This means that the counting process was stopped when the number of corrosion spots reached this value. Photographic images were taken on all samples for analysis with a Nikon D300S camera equipped with a Micro Nikkor objective with a focal length of 105 mm and an aperture of 1:2.8 inside of a light insulated casing and a white illuminated background.

2.3.3. Edge corrosion penetration

Edge corrosion starting from the original and cut edges was determined separately. The deepest penetration length, counted from the sample edge, was determined by simple manual measurements with a ruler or caliper. According to UNE 206016, the results of the cut edges were ignored for the evaluation of the material durability, but registered separately for reporting.

3. Results and discussion

In the following, the results of the six accelerated aging tests are presented. First, a general overview of the main results is given, then the influence of the tests on the specific degradation parameters is analyzed and the implications are discussed. Finally, a comparison of the required minimum testing times depending on degradation parameter and test is presented and evaluated. In this last paragraph a detailed evaluation is presented in which the necessary minimum testing durations are determined to provoke considerable, detectable degradation depending on the test and degradation parameter.

3.1. General observations

As it is the first time that results of tests with such long durations are presented, some remarkable general observations can be made regarding the extent of degradation suffered in the different tests. One of the main striking outcomes of the results achieved during this experimental campaign is the extreme aggressiveness of the CASS test in comparison with the other tests. The CASS test is the only one of the six tests that provokes corrosion in a reasonably short time and to a very considerable extent. Indications of considerable degradation of solar reflectors [13,47] and other coated metallic materials [48] in the CASS were found in the past. Fig. 1 represents one example of this highlight, where the pictures of RLA4 samples (which is a low-cost material prototype) submitted to all tests are shown after 480 h of testing or the next available testing time for the respective test, as pictures were not taken

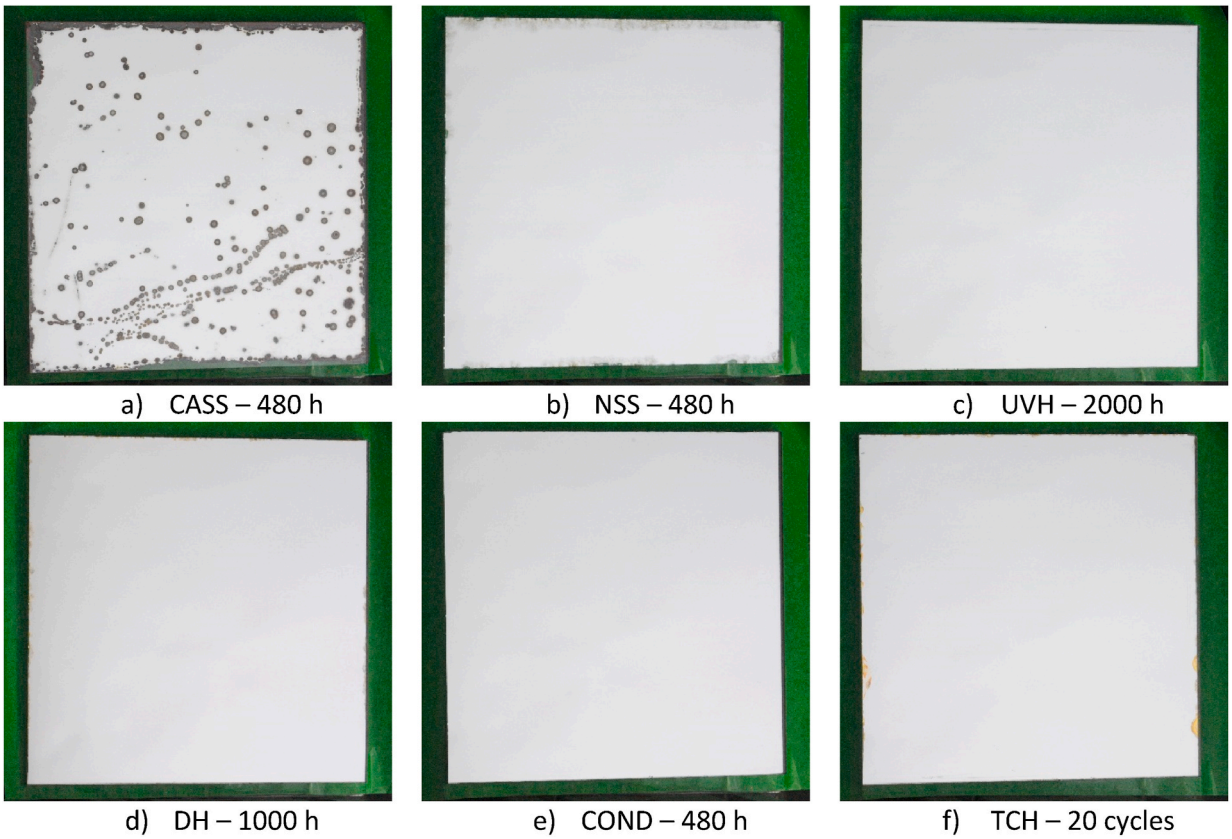

Fig. 1. Images of sample surface, material RLA4, all tests after 480 h or closest available duration to 480 h.

with the same frequency for all test in the case of insignificant corrosion. In these pictures, it can be seen that the CASS test produces significantly higher degradation due to corrosion of the silver layer than the rest of the tests. It is also remarkable that, at comparable durations, even weak materials such as the RLA4 show little degradation in the other tests.

Due to the strong degradation of most of the samples, the CASS testing was stopped after 2280 h instead of the 6000 h conducted for the other tests. Corrosion spots develop during the CASS for certain materials within hundreds of hours, reaching a far higher extent and covering a more important fraction of the reflector area, than in any other test even after much longer test durations. Some materials did not even reach the 2280 h in the CASS due to complete degradation. It also deserves to be mentioned that the aggressiveness of the CASS test does not affect all material tested in the same manner. See an example of the comparison of two materials with lower and higher degradation in Figs. 2 and 3 to observe the significant differences in the extension of the corrosion achieved during the CASS test. According to these results, it can be concluded that the CASS test is the best experiment to identify weak materials in very short times. Therefore, performing this test might be a suitable approach to avoid that non-proper materials enter the market.

Another general observation is that other tests, mainly the UVH and COND, cause an important number of corrosion spots after long test durations, but with spot sizes not exceeding a few hundred micrometers and thus covering only minimal parts of the surface. The small size of the corrosion spots in these tests causes problems in the detection of the defects, which are in part not detectable on images taken with the laboratory photographic equipment, but only by naked eye control and microscopic techniques (see example in Fig. 1c and d).

Finally, some of the tests provoke considerable corrosion of the unprotected edges but only minimal corrosion of the original edges (see example in Fig. 1 b). This means that the original edge protection is working properly and the results of this kind of tests with small samples might be unrealistic due to the unprotected edges influence.

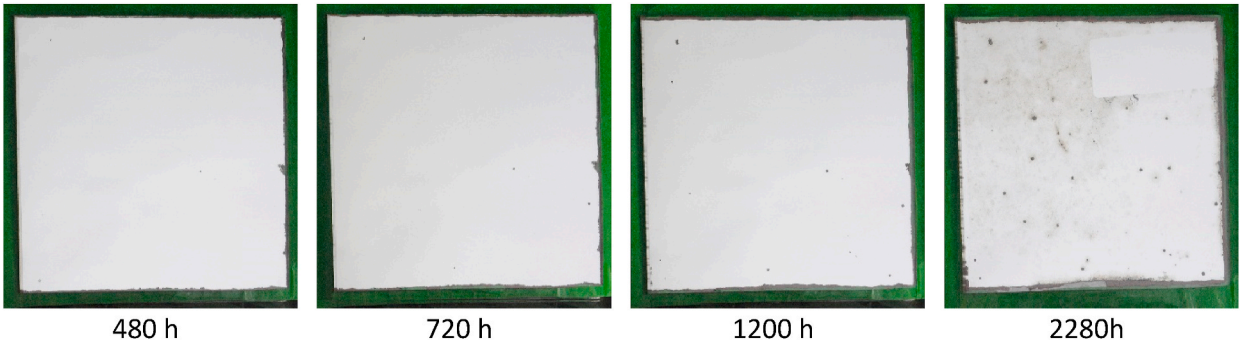

Fig. 2. RLA1R material in CASS test after 4 test times, final duration is last measurement taken before total degradation.

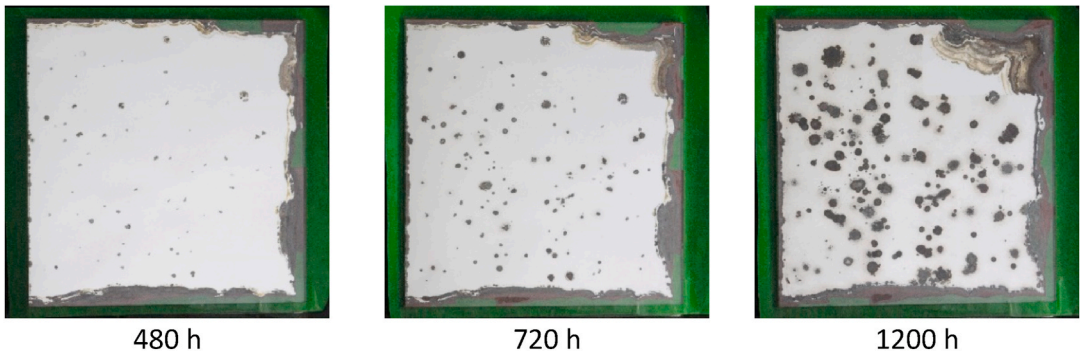

Fig. 3. RLA4R material in CASS test after 3 test times, final duration is last measurement taken before total degradation.

3.2. Reflectance

In this section, the results of the reflectance measurements are presented. Measured $\Delta\rho_{\lambda,\varphi}$ and $\Delta\rho_{s,h}$ are in general rather low. Exceptions are the CASS test, due to the large area fraction affected by corrosion, and the tests where glass corrosion is detected (mainly NSS and COND). In the other cases, the reflectance reduction stays far below 1 %.

As mentioned before, the highest reflectance losses are reached in the CASS test. Consequently, a thorough analysis of the results obtained in this test is presented first. The evolution of the $\Delta\rho_{\lambda,\varphi}$, over testing time for all materials in the CASS test is displayed in Fig. 4 left, where it can be seen that the reflectance considerably decreases for all materials, except RLA3. Strong differences in the behavior can be seen between materials, but a typical tendency in the curves is observed, namely, reflectance remains unaltered until a certain moment, when it sharply decreases. This abrupt decrease starts in RLA4 already after less than 500 h, and consecutively later for other materials, with materials RLA1 and RLA1R resisting until nearly 2000 h. RLA3 is the only material in this test which shows only marginal losses until the end of the test. One remarkable observation is that after 120 h, the minimum duration recommended in the UNE 206016 standard, only marginal losses were detected in all materials, as can be seen in a zoom of the same graph, in Fig. 4 right. This means that it is intensely recommended to conduct the CASS test for longer duration than the minimum suggested.

The reflectance loss of the materials is directly connected to the development of corrosion in the silver layer. This can be seen by comparing the reflectance loss evolution to the equivalent formation of silver corrosion spots, discussed in the next section. An example of the importance of the magnitude of the corrosion spots can be observed in Fig. 5, which shows the evolution of the corrosion spots on a material RLB3 sample during CASS from 480 h to 720 h. This corresponds to the period in which the strong growth of corrosion spots starts to develop and at the same time the reflectance starts to decrease abruptly (see Fig. 4 left). As the reflectance measurements were supposed to be taken on uncorroded areas, considerable changes in reflectance are detected as soon as the density of the corrosion spots reaches values too high to allow for the proper measurement on uncorroded areas. The used equipment for the reflectance measurement cover only measurement spots not exceeding 1–2 cm^2 and thus even with several measurements on the samples used during the tests, only a small part of the sample surface is covered. An equipment covering the whole sample or bigger parts of the surface would benefit the measurement. For the CASS, the measurements are performed every 120 h and significant changes can be seen between consecutive measurements. This fact highlights the importance of intermediate measurements during testing and the selection of an adequate measurement frequency. Depending on the aggressiveness of the tests and the expected amount of degradation, an appropriate frequency for the analysis, not only for the reflectance measurements, may be chosen to not miss important steps in the degradation evolution. If only a pass/fail test at one predetermined test duration is of interest or only marginal degradation is expected, the intermediate measurements may be omitted.

With respect to the other tests, the corrosion of the glass surface is provoking considerable reflectance reductions for some materials in the NSS and the COND tests. In Fig. 6, the reflectance drop is displayed over test time in the NSS (left graph) and COND (right graph) tests. Glass corrosion is a chemical attack of the glass surface connected to high humidity conditions [33]. Examples of this mechanism developing during NSS and COND are presented in Fig. 7, with microscopic images. It is an effect that is uncommonly encountered during outdoor exposure at normal operation and so far has only been detected for some specific conditions, such as close to the cooling towers of CST plants [49,50]. Therefore, and because it can have an important impact on reflectance, in accelerated tests the protection of the glass surface can be considered by the application of a suitable tape [43]. The application of protective tape on at least one of the tested samples is also recommended in UNE

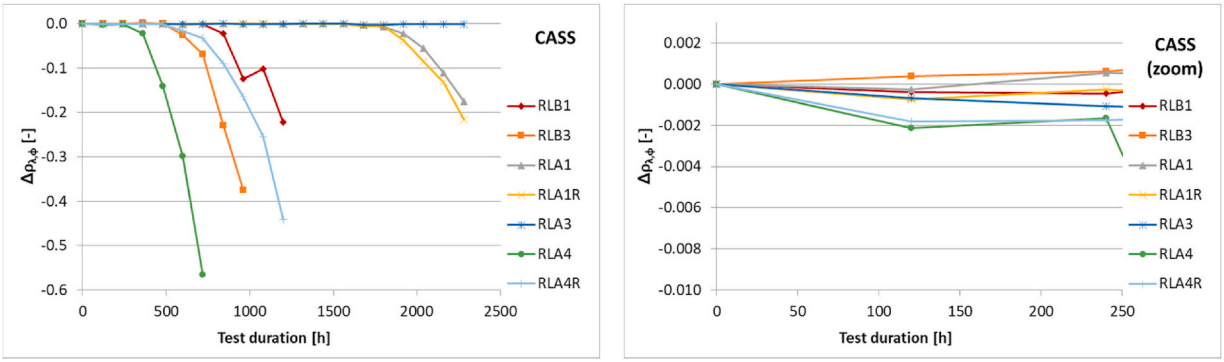

Fig. 4. Evolution of the $\Delta\rho_{\lambda,\varphi}$ for all materials in the CASS test. On the right, a zoom of the left graph is displayed, showing the reflectance changes during first 240 h of CASS test for all materials.

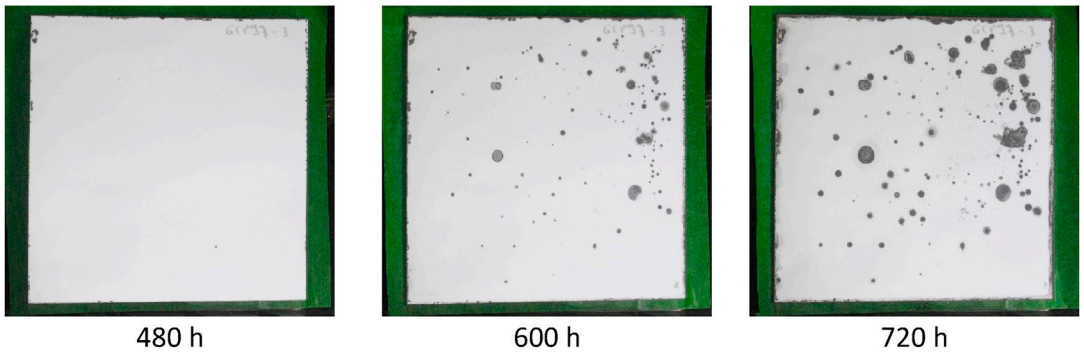

Fig. 5. Evolution of the corrosion spots on surface of RLB3 sample from 480 h to 720 h, the period in which strong growth of spots and strong decay of reflectance is registered.

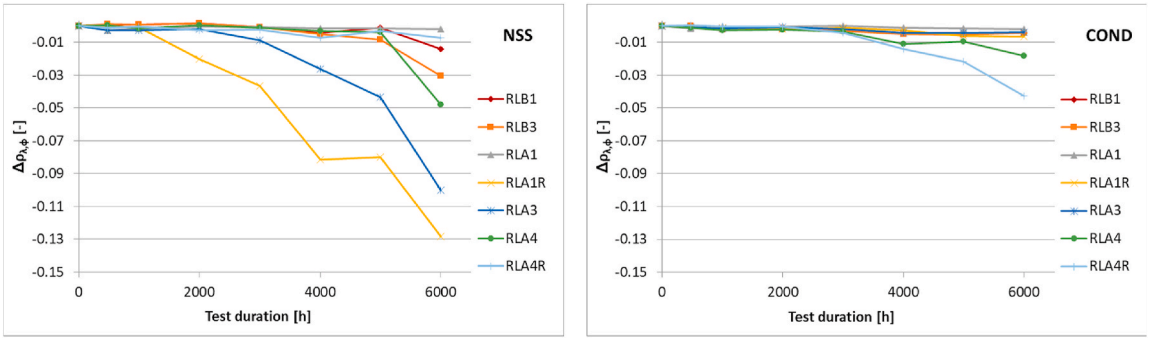

Fig. 6. Evolution of the $\Delta\rho_{\lambda,\varphi}$ for all materials, averaged for the three sample tested (that is, with and without protective tape). Each figure corresponds to a different accelerated aging test, being left for CASS and right for COND.

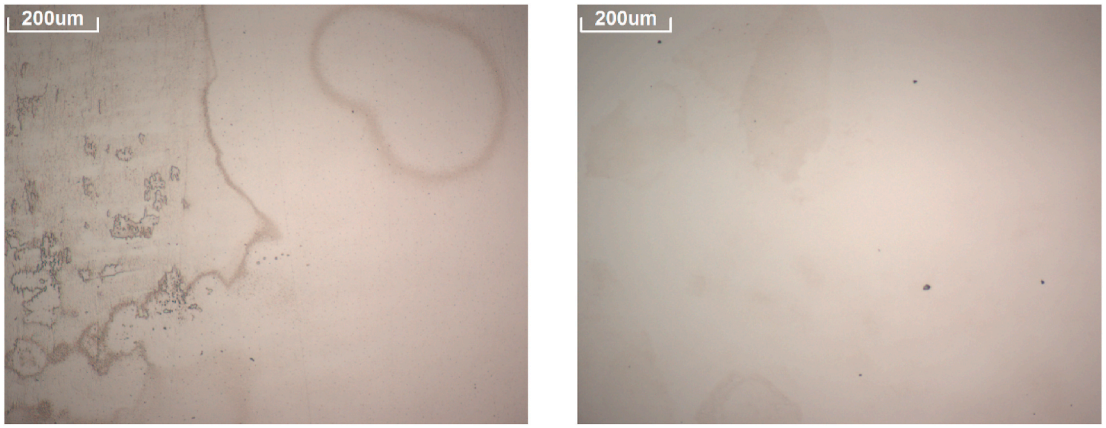

Fig. 7. Microscopic images of glass surface presenting glass corrosion, for RLA1R material after 6000 h of NSS tests (left) and RLA4R material after 6000 h of COND test (right).

206016.

As the glass corrosion is considered an effect that is not provoked under most realistic outdoor exposure conditions, the $\Delta\rho_{\lambda,\varphi}$ results of only the samples protected with a tape of the NSS and COND test are presented in Fig. 8. These are the samples representing typical operating conditions to be properly compared with the rest of tests. In the latter case (UVH, DH and TCH tests) the average of the 3 samples tested are considered, because they are not affected by glass corrosion. The evolution of the reflectance of the remaining tests, together with the taped samples of NSS and COND test in Fig. 8, is minimal, considering the different scale of the graphs compared to Figs. 4 and 6. The reflectance decrease does not exceed 1 % and is limited in most cases even to values around 0.5 pp or lower, close to the uncertainty of the measurement equipment [46]. Due to the lack of changes in the material, not all intermediate measurements were performed for the TCH test. In the evolution of the materials, even an increase in reflectance was measured from time to time. This uncertainty in the measurements is mainly caused by unavoidable differences in the calibration of the equipment and possibly also by varying effectiveness of the cleaning of the reflector surface of residues from the different tests [18,51]. These residues may not significantly alter the perception of the sample optical quality but lead to minimal decrease in reflectance. This is why, especially for long term tests with little reflectance differences, rigorous cleaning, if necessary with solvents like isopropanol or acetone, is recommended [52,53]. The clearest downward trend for these tests is detected in the DH with a maximum decrease of ca. 0.8 pp. and to a lower extend in the

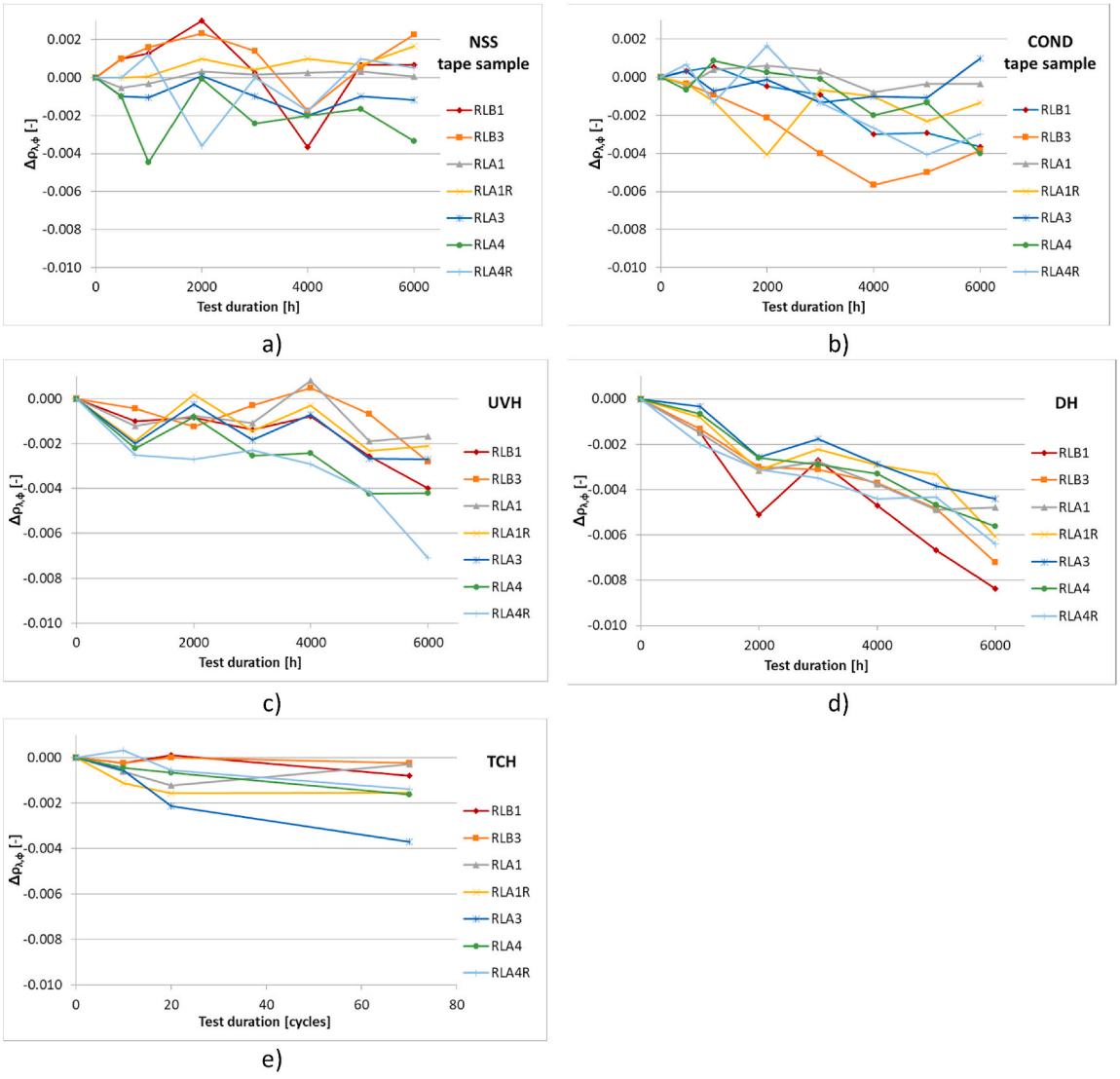

Fig. 8. Evolution of the $\Delta\rho_{\lambda,\varphi}$ for all materials, averaged for the three sample tested (that is, with and without protective tape), except in the NSS and COND tests, where only samples with protective tape are included. Each figure corresponds to a different accelerated aging test, being a) for NSS, b) for COND, c) for UVH, d) for DH and e) for TCH.

UVH and TCH test. A combination of beginning corrosion and residues on the surface is most likely to play a role here.

Measurements of the $\Delta\rho_{s,h}$ evolution were performed as well, but are not presented here in detail. The reason is that the $\Delta\rho_{s,h}$ follow the same tendency as the $\Delta\rho_{\lambda,\varphi}$ for all materials and tests, but to a lower extent. Final $\Delta\rho_{\lambda,\varphi}$ and $\Delta\rho_{s,h}$ are displayed in Table 3, representing the mean values of all materials per test and including all samples (with and without tape). Additionally, the results of the samples with tape for NSS and COND tests are shown. Results for the CASS test are not included in the table, because total test duration differs between materials and reflectance reached values close to zero due to nearly complete degradation after different durations for different materials. For the last measurements before total degradation in the CASS, reflectance decays of over 50 % were registered in extreme cases. In the table, it can be seen that for the samples without glass corrosion, $\Delta\rho_{\lambda,\varphi}$ and $\Delta\rho_{s,h}$ are very similar. The samples including the glass corrosion show much stronger differences for the specular values. This is due to the fact that many degradation mechanisms increase the scattering of light, which has a stronger influence on the specular reflectance [26,54]. $\rho_{\lambda,\varphi}$ measurements are therefore more sensitive to detect degradation, while $\rho_{s,h}$ measurements are mainly important to detect changes in the spectral behavior of the reflectance.

Table 3
Mean final reflectance differences by test for all materials, specular and solar-weighted hemispherical, after 70 cycles for the TCH test and 6000 h for the rest of the tests.

Test (material)	$\Delta\rho_{\lambda,\varphi}$ [−]	$\Delta\rho_{s,h}$ [−]
NSS (all)	−0.047 ± 0.049	−0.012 ± 0.015
NSS (tape samples only)	0.000 ± 0.002	0.000 ± 0.001
COND (all)	−0.012 ± 0.015	−0.004 ± 0.002
COND (tape samples only)	−0.002 ± 0.002	−0.003 ± 0.002
TCH (all)	−0.001 ± 0.001	−0.001 ± 0.001
UVH (all)	−0.004 ± 0.002	−0.003 ± 0.002
DH (all)	−0.006 ± 0.001	−0.006 ± 0.002

3.3. Silver-corrosion spots

In Fig. 9, the evolution of the d_{corr} is displayed for all tests and materials. The density of 1/cm^2 corresponds to the maximum counted of 100 spots per (10 × 10 cm^2) sample. This value is only reached for some materials in the CASS test (RLB1, RLB3, RLA4 and RLA4R) and one

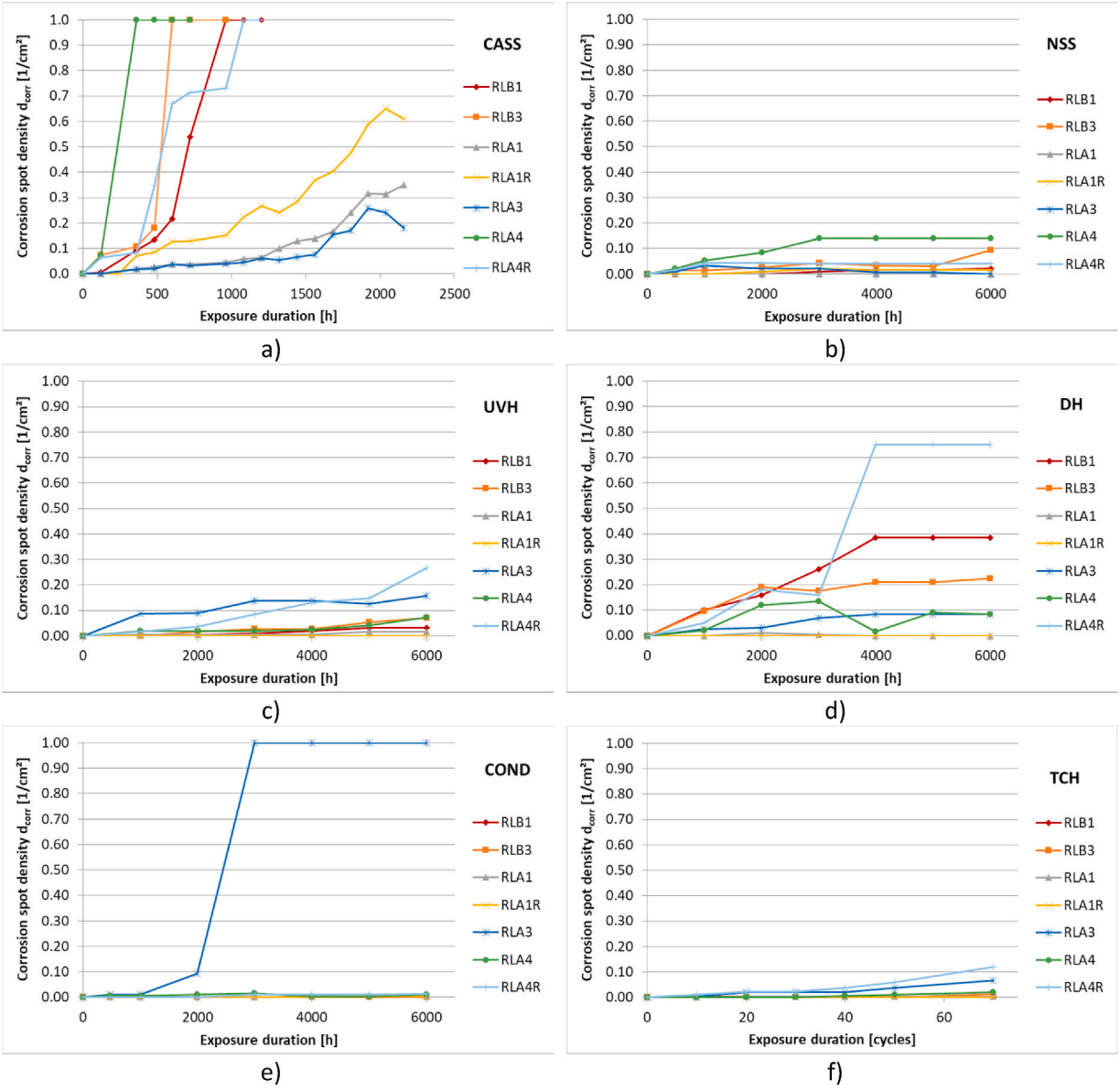

Fig. 9. Evolution of d_{corr} for all materials and tests. Each figure corresponds to a different accelerated aging test, being a) for CASS, b) for NSS, c) for UVH, d) for DH, e) for COND and f) for TCH.

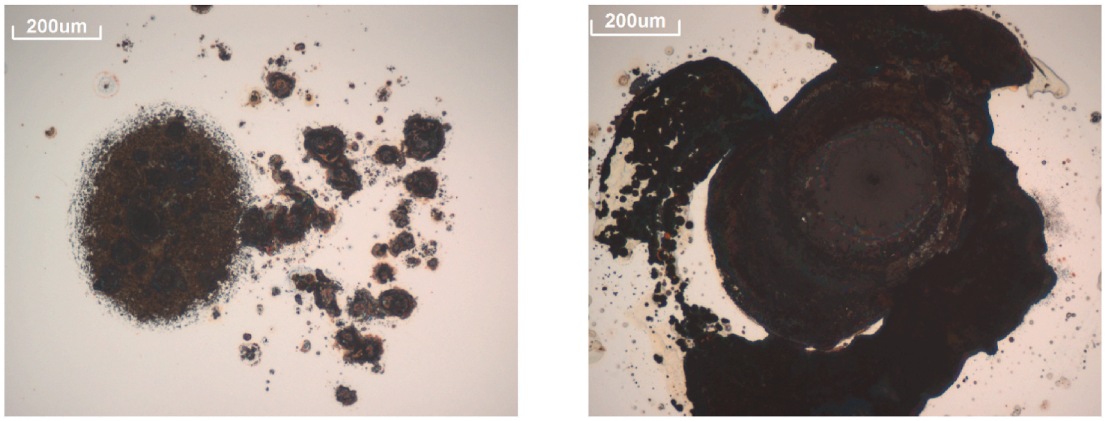

Fig. 10. Microscopic images of medium size corrosion spots after CASS testing, left: material RLA1 after 480 h, right: RLA4 after 320 h.

material in the COND test (RLA3). As for the reflectance data, here the extreme aggressiveness of the CASS compared to the other tests is clear. The test provokes the highest number of spots and does so in a relatively short time. For certain materials in the long duration corrosive tests, especially the NSS, only a small area remains available for analysis of spot creation because of the reduction of the area by excessive edge corrosion (see next section).

Some other tests, mainly the DH and to a lesser extent the COND and UVH tests, provoked a considerable number of spots after a longer test duration. The main difference here is in the size of the corrosion spots. While in the CASS test the corrosion spots reach a considerable size and for certain materials cover an important fraction of the surface, the spots in the other tests remain mostly very small (<1 mm). See Fig. 1 for comparison of the spots developing in the CASS test in relation to the other tests. In Fig. 10 exemplary microscopic images are displayed of typical medium size (ca. 1 mm diameter) corrosion spots developing during CASS test. Usually these spots grow further [55], far exceeding this microscopic level and covering considerably larger areas.

Furthermore, as an example, images of samples with a high number of extremely small corrosion spots after 6000 h of DH and COND tests are displayed in Fig. 11 and can be compared to Figs. 1–3 for the CASS case. At times, spots in DH, UVH and COND even cannot be detected with the currently used camera system in the laboratory, because they are too small in size (not exceeding a few hundred micrometers) or because the silver is not completely corroded in the spots, resulting in lower brightness contrast. Naked-eye counting allows the detection of this type of spots, but faces its limits when reaching a high spot density, which makes the accurate counting impossible [13,56]. In addition, this technique is much dependent on the user and observation conditions (e.g. lighting). Microscopic techniques can be used to check sizes of individual spots and to determine a spot density in cases of very high densities, but need to reach a high enough surface coverage with high magnifications [57,58]. Microscopic images of spots in DH and COND are displayed in Fig. 12. The determination of the degraded area with automatic image analysis techniques can be of interest to calculate its influence on the reflectance, but especially in the cases of small spots, it depends on the image resolution and further parameters as illumination and the applied thresholds for analysis. A standard for this technique is not available so far and results should be checked, e.g. by comparison with microscopic images. Depending on the use case of the conducted test campaign, the importance of the selected parameters may differ, e.g. the affected area gives a direct indication on the reflectance loss while the density of spots allows predictions of the potential future reflectance loss due to the growth of the created spots.

3.4. Edge corrosion

Corrosion of the silver layer can start from the edges of the samples and penetrate further into the sample surface. Usually, only the edge corrosion starting at the original, meaning not cut, edges of the samples is taken into consideration for evaluation of the degraded area. Real commercial facets always have their edges protected during the production process, which doesn't leave the silver layer exposed to the environment [59]. For testing purposes, samples are often cut from facets and possess original and cut edges. The cut edges are usually more prone to corrosion and the development of this kind of corrosion gives only debatable indication of the materials durability and is therefore omitted for the analysis. In the current research work, original edge corrosion was not detected in most of the materials and tests and only developed during two of the tests, the CASS and the NSS tests. See the evolution of the original edge penetration for both tests in Fig. 13, on the left for CASS and on the right for NSS. As for the other parameters, the CASS is the most aggressive test. Important differences in the original edge corrosion evolution exist between materials and not all materials were affected. Due to the manual measurement procedure with its uncertainties, at times the corrosion penetration shows small decreases for certain samples. Again an automated image processing procedure for the analysis could improve the situation.

In all cases, the cut edge corrosion is much more pronounced than the original edge corrosion. In Fig. 14 left, an example can be seen with a sample after 2000 h of NSS testing with the uncorroded original edge on the right side. However, the cut edge corrosion for certain samples reaches such a magnitude, that only a small portion of sample surface remains (as can be observed in Fig. 14 right), which makes the evaluation of other parameters difficult. To avoid an excessive corrosion of the sample surface through the cut edges, a proper protection, i.e. with special tapes or lacquers [60], should be applied prior to the testing.

The evolution of the cut edge corrosion penetration is displayed in Fig. 15 for the tests in which penetration is considerable, here selected over 0.5 cm. Development is much stronger in the corrosive tests, CASS and NSS. In the TCH test, the effect is accompanied by a complete peeling of the reflective and paint layers in the affected region. After 10 to 20 cycles, a saturation is reached and penetration does not grow considerably with longer testing time (see example in Fig. 16, where the state of a sample is compared after 20 and 70 cycles).

3.5. Comparison of parameters and tests

An overview graph was created to be able to quickly evaluate the behavior of the parameters in the different tests and to compare the required minimum testing time to detect differences between materials. All presented parameters and tests are evaluated and the minimum testing time in which one of the materials shows considerable growth of the respective parameter is recorded. Limits for what is regarded as considerable have to be established for that. For the corrosion parameters, any detected growth is taken into consideration. For the reflectance

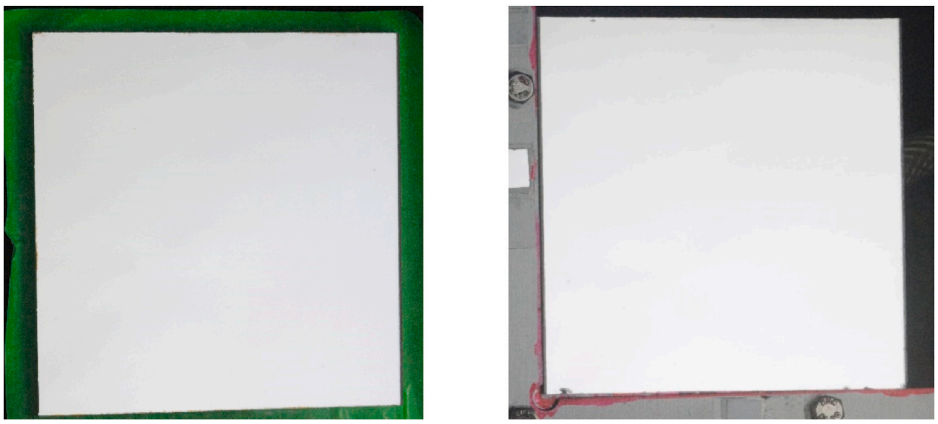

Fig. 11. Photographic images of the whole sample surfaces. Left: RLA4R sample after 6000 h of the DH test; Right: RLA3 sample after 6000 h of the COND test.

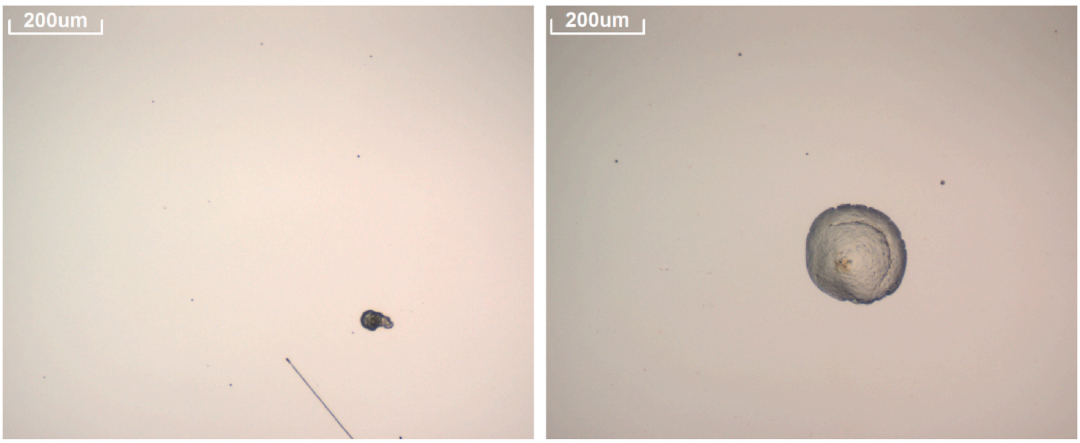

Fig. 12. Microscopic images of the extremely small defects in reflective silver layer. Left: RLA4R sample after 6000 h of DH test; Right: RLA3 sample after 6000 h of COND test.

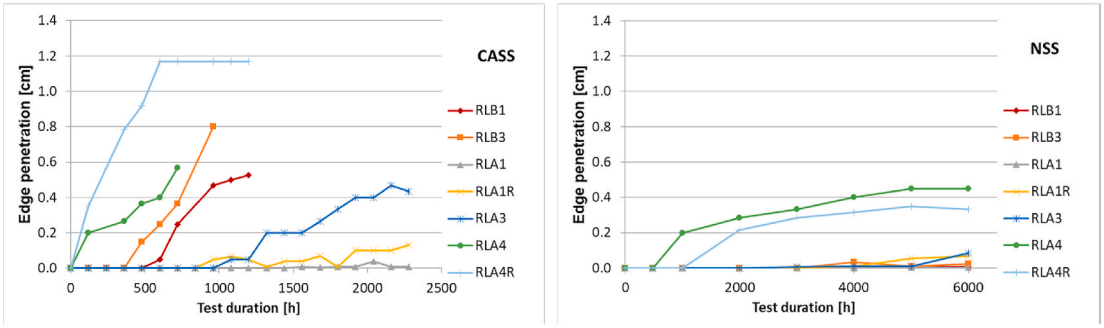

Fig. 13. Evolution of the original edge corrosion penetration for all materials. Each figure corresponds to a different accelerated aging test, being left for CASS test and right for NSS test.

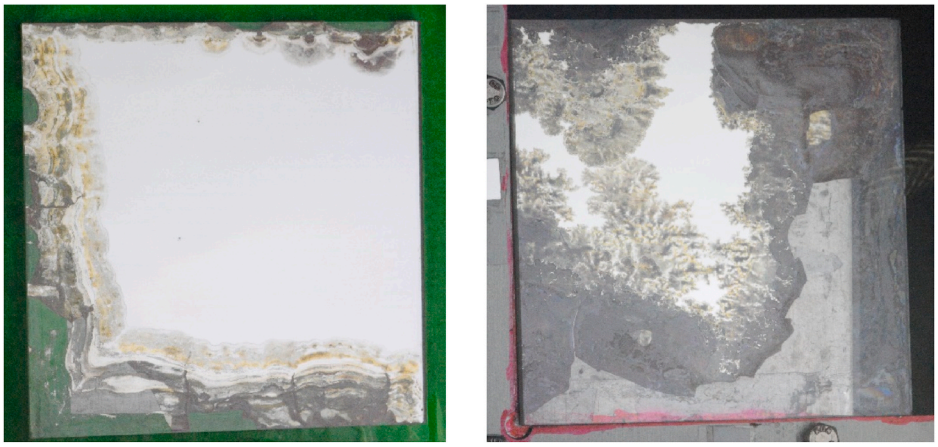

Fig. 14. Images of front side of material RLA4R after 2000 h of NSS test(left) and material RLA3 after 6000 h of NSS test (right). In both cases, the right edge being the original one.

parameters, the respective uncertainties are selected, 0.003 for the $\rho_{\lambda,\varphi}$, and 0.008 for the $\rho_{s,h}$.

The resulting graph is displayed in Fig. 17, where the data is grouped by parameter and within each parameter group, every bar represents one test. Grey bars represent cases in which minimum growth is not reached until completion of the test. From the graph, it is clear that the spot density is the parameter which reaches differences between materials with the lowest testing time. The second parameter is the cut edge corrosion, but as mentioned earlier, correlation with real-exposure degradation is questionable. Regarding reflectance, the $\rho_{\lambda,\varphi}$ shows results after a reasonable time, which is clearly lower than for the $\rho_{s,h}$. To provoke differences for the $\rho_{s,h}$, durations of 4000 h and higher are necessary. Finally, original edge-corrosion is the least sensitive parameter and in 4 out of 6 tests does not reach the threshold for any of the materials. With these results it is possible to estimate reasonable durations for the different tests.

Comparing the different tests, again, the aggressiveness of the CASS is clearly visible resulting in the lowest minimum testing times for all

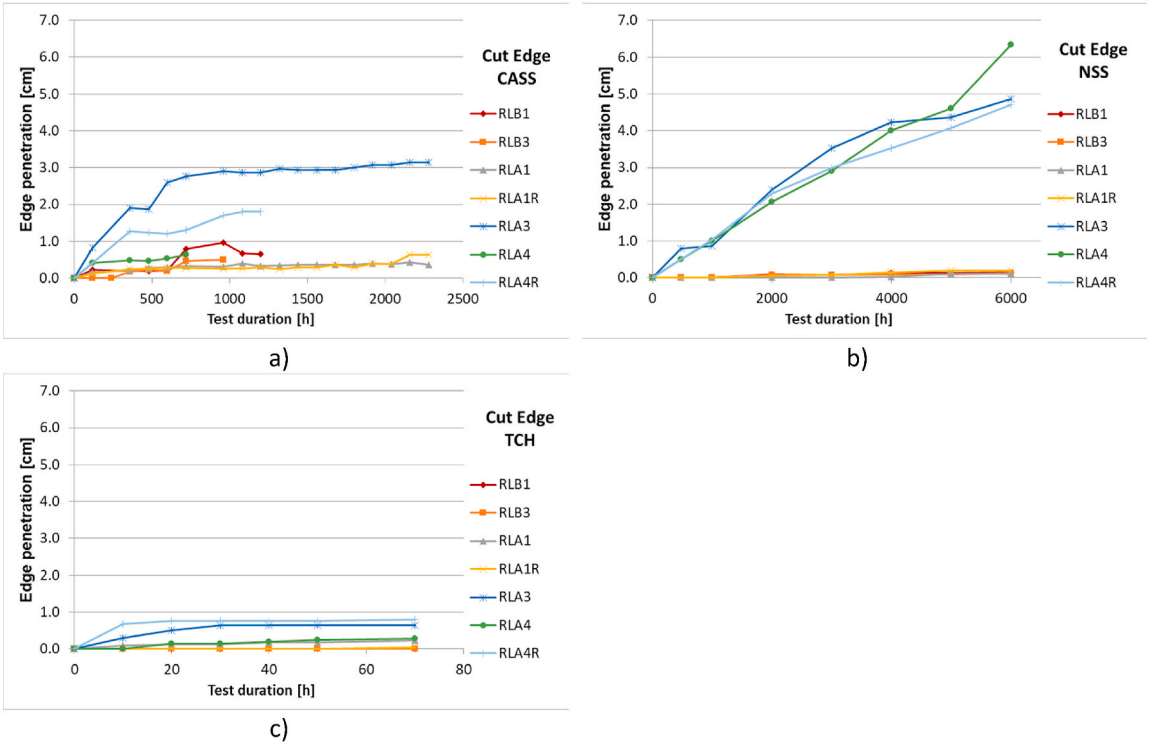

Fig. 15. Evolution of the cut edge corrosion penetration for all materials in CASS, NSS and TCH tests. Each chart corresponds to a different accelerated aging test, being a) for CASS test, b) for NSS test and c) for TCH test.

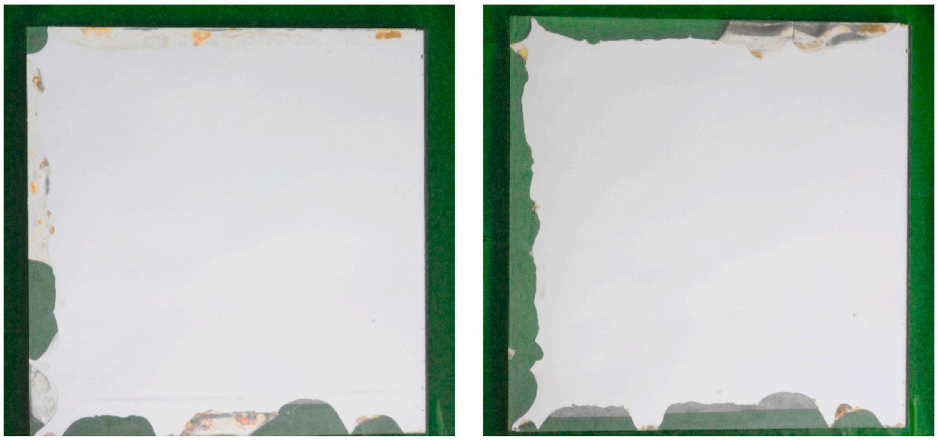

Fig. 16. Images of sample surface material RLA4 after 2 test durations in TCH, 20 cycles (left) and 70 cycles (right) with resulting edge peeling.

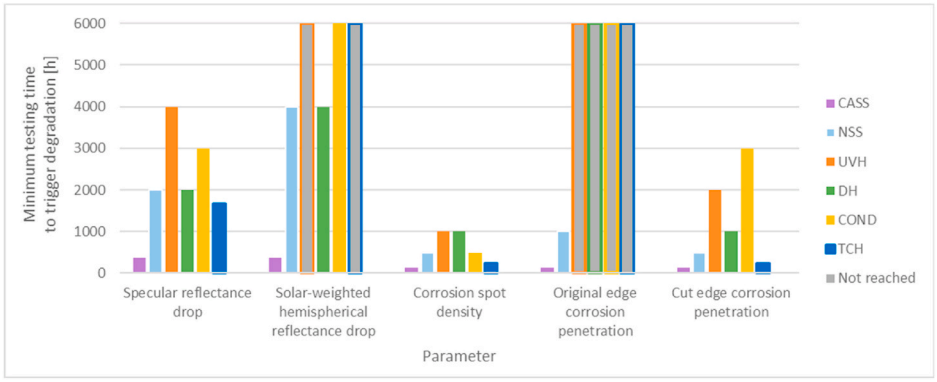

Fig. 17. Comparison of required testing time to reach detectable differences between materials depending on parameter and test.

parameters (purple bars in Fig. 17). After 360 h, all parameters reveal differences and much longer testing times may not be needed. For the other tests, testing times of ca. 1000 h may be appropriate if the corrosion parameters are evaluated, but longer testing times are necessary to be significant for the reflectance parameters.

The minimum testing times to trigger measurable degradation of the here presented graph may look different for mirror materials from other manufacturers, but this graph may serve as a valuable tool to choose tests and evaluation parameters. Depending on specific test objectives, also the thresholds for what is counted as significant degradation may be adapted. The information on the tests and parameters is intended to design future test campaigns properly and to exploit their results for their further use, such as the evaluation of novel materials and the development of degradation models, correlations to outdoor behavior and lifetime prediction procedures.

4. Conclusions

Several important conclusions can be drawn about the measurement parameters and their determination as well as the execution and interpretation of the typical accelerated aging tests. Even though agreement on the ideal parameters to be determined for the evaluation of the degradation of solar reflectors has not been reached until today, important recommendations can be extracted from the results of the experiments performed in this investigation.

First of all, the measurement of the reflectance as the determining parameter for the durability of the reflectors has its shortcomings. No commercial equipment is available on the market for space resolved measurements or to determine the $\rho_{s,\varphi}$. Nowadays the use of the combination of spectrophotometer and reflectometer measurements gives the minimum information necessary for the evaluation. During the here conducted campaign, differences manifest quicker and stronger in specular values compared to hemispherical ones. In the case of inhomogeneous ρ over the sample surface, the measurements should be combined with the determination of the degraded area and the increase of the number of measurements per sample. During the execution of the current long duration tests, the detected differences in $\rho_{s,h}$ are rather low except for CASS, but below the uncertainty for the UVH and TCH tests even after 6000 h. To detect small differences in the NSS, COND and DH tests, appropriate cleaning has to be applied, to avoid fluctuations in the measurements due to residues. Prevention of undesired effects, such as glass corrosion, e.g. by application of protective tape, is necessary. In the case of the more aggressive tests, intermediate measurements are recommended to detect progressive changes in the sample characteristics.

The d_{corr} is the parameter that yields changes for different materials in all tests with the lowest required test time. The determination of the degraded reflective area, by corrosion spots or edge corrosion, is as challenging as the measurement of the reflectance. The recommended counting by naked eye is feasible for a low number of spots with relatively large size (diameter >200 μm) but more automated techniques should be investigated and applied, such as automatic image treatment of photographic or microscopic images. For the evaluation of a reflector material, the affected size as well as the number of spots are interesting. The affected area because it directly reduces the mean reflectance of the sample and the number of spots because they may indicate the future change in reflectance due to a possible growth of these spots.

Corrosion penetrating from the edges has to be divided between original and cut edges and developed in the most aggressive tests. The cut edge corrosion develops quicker and can be used for comparison between materials, but its final significance has to be proven. Adequate edge sealing is recommended to avoid an excessive loss of reflective area due to cut edge corrosion.

Comparing the different tests, further conclusions can be drawn. The CASS is the most aggressive test and serves as quick way to provoke degradation and to compare different materials. Although the minimum duration of the CASS test suggested in the UNE 206016 standard (that is, 120 h) is clearly insufficient, after 360 h of testing all parameters show differences. Therefore, an appropriate duration of the CASS test has to be selected to obtain enough useful information but avoiding excessive and possibly unrealistic degradation. The other tests have provoked only very minor degradation. In this campaign 1000 h of testing in the remaining tests are enough to provoke detectable corrosion, but longer times may be needed to see changes in reflectance. In general, longer test time compared to available standards are recommended, unless the materials investigated are of very low durability or special weaknesses (e.g. UV sensitive paints, flaking in thermal cycles) are expected.

CRediT authorship contribution statement

Johannes Wette: Writing – original draft, Visualization, Methodology, Investigation, Formal analysis, Data curation. **Florian Sutter:** Supervision, Methodology, Investigation, Data curation, Conceptualization. **Ricardo Sánchez-Moreno:** Project administration, Methodology, Investigation. **Florian Wiesinger:** Validation, Investigation, Data curation. **Aránzazu Fernández-García:** Writing – review & editing, Supervision, Project administration, Methodology, Investigation, Funding acquisition, Formal analysis, Conceptualization.

Declaration of competing interest

The authors declare that they have no known competing financial interests or personal relationships that could have appeared to influence the work reported in this paper.

Data availability

Data will be made available on request.

References

[1] World Energy Outlook 2023, IEA, 2023.
[2] K. Ardani, P. Denholm, T. Mai, R. Margolis, E. O'Shaughnessy, T. Silverman, J. Zuboy, Solar Futures Study, US Department of Energy, USA, 2021.
[3] La industria termosolar como motor económico en España, Protermosolar, 2021.
[4] Renewable Energy Storage Roadmap, CSIRO, 2023.
[5] G. Zhu, C. Augustine, R. Mitchell, M. Muller, P. Kurup, A. Zolan, S. Yellapantula, R. Brost, K. Armijo, J. Sment, R. Schaller, M. Gordon, M. Collins, J. Coventry, J. Pye, M. Cholette, G. Picotti, M. Arjomandi, M. Emes, D. Potter, M. Rae, Roadmap to advance heliostat technologies for concentrating solar-thermal power. https://doi.org/10.2172/1888029, 2022.
[6] CSP. guru, A Database of Concentrating Solar Power Plants of the World for Energy Modellers and Analysts. (n.d.). https://csp.guru//(accessed January 15, 2024).
[7] T. Fend, B. Hoffschmidt, G. Jorgensen, H. Küster, D. Krüger, R. Pitz-Paal, P. Rietbrock, K.-J. Riffelmann, Comparative assessment of solar concentrator materials, Sol. Energy 74 (2003) 149–155, https://doi.org/10.1016/S0038-092X(03)00116-6.
[8] B. Bierman, J. O'Donnell, R. Burke, M. McCormick, W. Lindsay, Construction of an enclosed trough EOR system in south Oman, Energy Proc. 49 (2014) 1756–1765, https://doi.org/10.1016/j.egypro.2014.03.186.
[9] P. Forman, S. Penkert, A. Pfahl, J. Schnell, P. Mark, Development of a modular concrete heliostat prototype, AIP Conf. Proc. 2445 (2022) 120013, https://doi.org/10.1063/5.0086016.
[10] Michael DiGrazia, Gary Jorgensen, Reflectech mirror film: design flexibility and durability in reflecting solar applications, in: Proceedings of the 39th ASES National Solar Conference 2010, 2010. Phoenix.
[11] F. Sutter, A. Fernández-García, P. Heller, K. Anderson, G. Wilson, M. Schmücker, P. Marvig, Durability testing of silvered-glass mirrors, Energy Proc. 69 (2015) 1568–1577, https://doi.org/10.1016/j.egypro.2015.03.110.
[12] F. Buendía-Martínez, F. Sutter, J. Wette, L. Valenzuela, A. Fernández-García, Lifetime prediction model of reflector materials for concentrating solar thermal energies in corrosive environments, Sol. Energy Mater. Sol. Cell. 224 (2021) 110996, https://doi.org/10.1016/j.solmat.2021.110996.
[13] F. Sutter, A. Fernández-García, J. Wette, T.J. Reche-Navarro, L. Martínez-Arcos, Acceptance criteria for accelerated aging testing of silvered-glass mirrors for concentrated solar power technologies, Sol. Energy Mater. Sol. Cell. 193 (2019) 361–371, https://doi.org/10.1016/j.solmat.2019.01.008.
[14] UNE, UNE 206016, Reflector Panels for Concentrating Solar Technologies, UNE, Madrid, 2018.
[15] F. Sutter, A. Fernández-García, J. Wette, F. Wiesinger, Assessment of durability and accelerated aging methodology of solar reflectors, in: The Performance of Concentrated Solar Power (CSP) Systems: Analysis, Measurement and Assessment, 2017, pp. 169–201, https://doi.org/10.1016/B978-0-08-100447-0.00006-7.

[16] F. Wiesinger, F. Sutter, A. Fernández-García, J. Wette, N. Hanrieder, Sandstorm erosion on solar reflectors: a field study on height and orientation dependence, Energy 217 (2021) 119351, https://doi.org/10.1016/j.energy.2020.119351.
[17] V.L. Morris, Cleaning agents and techniques for concentrating solar collectors, Sol. Energy Mater. 3 (1980) 35–55, https://doi.org/10.1016/0165-1633(80)90048-9.
[18] C. Sansom, A. Fernández-García, F. Sutter, H. Almond, P. King, L. Martínez-Arcos, Soiling and cleaning of polymer film solar reflectors, Energies 9 (2016), https://doi.org/10.3390/en9121006.
[19] IEC 62108:2022, Concentrator Photovoltaic (CPV) Modules and Assemblies - Design Qualification and Type Approval, 2022.
[20] T. Farrell, Y. Cao, F. Burkholder, D. Celvi, C. Schreiber, G. Zhu, Compilation of a solar mirror materials database and an analysis of natural and accelerated mirror exposure and degradation, J. Sol. Energy Eng. 145 (2023), https://doi.org/10.1115/1.4063079.
[21] A. García-Segura, A. Fernández-García, M.J. Ariza, F. Sutter, T.C. Diamantino, L. Martínez-Arcos, T.J. Reche-Navarro, L. Valenzuela, Influence of gaseous pollutants and their synergistic effects on the aging of reflector materials for concentrating solar thermal technologies, Sol. Energy Mater. Sol. Cell. 200 (2019), https://doi.org/10.1016/j.solmat.2019.109955.
[22] A. Grosjean, E. Le Baron, A.-C. Pescheux, A. Disdier, Accelerated aging tests and characterizations of solar mirrors: comparison of combinations of stress factors on degradation, Sol. Energy Mater. Sol. Cell. 220 (2021) 110851, https://doi.org/10.1016/j.solmat.2020.110851.
[23] J. Wette, F. Sutter, M. Tu, A. Fernández-García, F. Buendía, M.J. Carvalho, T. Diamantino, Advanced cyclic accelerated aging testing of solar reflector materials, AIP Conf. Proc. 2126 (2019) 160007, https://doi.org/10.1063/1.5117670.
[24] A. Fernández-García, L. Martínez-Arcos, F. Sutter, J. Wette, F. Sallaberry, R. Erice, T. Diamantino, M.J. Carvalho, O. Raccurt, A.-C. Pescheux, G. Imbuluzqueta, M. Machado, Accelerated aging test of solar reflectors according to the new AENOR standard – results of a round Robin test, Santiago, Chile, https://doi.org/10.1063/1.5067231, 2018.
[25] Agc - SunMax premium reflect - datasheet. https://www.agc-solar.com/wp-content/uploads/2022/01/Factsheets_SunMax-Premium-Reflect_0122_EN.pdf, 2022. (Accessed 16 July 2024).
[26] F. Sutter, A. Fernández-García, M. Montecchi, Indirect method to determine near-normal sun-conic reflectance, Daegu, South Korea (2020) 100007, https://doi.org/10.1063/5.0028749.
[27] M. Montecchi, Proposal of a new parameter for the comprehensive qualification of solar mirrors for CSP applications, AIP Conf. Proc. 1734 (2016) 130014, https://doi.org/10.1063/1.4949224.
[28] A. Heimsath, P. Nitz, Scattering and specular reflection of solar reflector materials – measurements and method to determine solar weighted specular reflectance, Sol. Energy Mater. Sol. Cell. 203 (2019) 110191, https://doi.org/10.1016/j.solmat.2019.110191.
[29] F. Sutter, A. Fernández-García, A. Heimsath, M. Montecchi, C. Pelayo, Advanced measurement techniques to characterize the near-specular reflectance of solar mirrors, AIP Conf. Proc. 2126 (2019) 110003, https://doi.org/10.1063/1.5117618.
[30] F. Sutter, S. Meyen, A. Fernández-García, P. Heller, Spectral characterization of specular reflectance of solar mirrors, Sol. Energy Mater. Sol. Cell. 145 (2016) 248–254, https://doi.org/10.1016/j.solmat.2015.10.030.
[31] M. Montecchi, Approximated method for modelling hemispherical reflectance and evaluating near-specular reflectance of CSP mirrors, Sol. Energy 92 (2013) 280–287, https://doi.org/10.1016/j.solener.2013.03.014.
[32] F. Buendía-Martínez, A. Fernández-García, F. Sutter, L. Valenzuela, A. García-Segura, Advanced analysis of corroded solar reflectors, Coatings 9 (2019), https://doi.org/10.3390/coatings9110749.
[33] A. García-Segura, F. Sutter, L. Martínez-Arcos, T.J. Reche-Navarro, F. Wiesinger, J. Wette, F. Buendía-Martínez, A. Fernández-García, Degradation types of reflector materials used in concentrating solar thermal systems, Renew. Sustain. Energy Rev. 143 (2021) 110879, https://doi.org/10.1016/j.rser.2021.110879.
[34] M. Brogren, B. Karlsson, A. Roos, A. Werner, Analysis of the effects of outdoor and accelerated ageing on the optical properties of reflector materials for solar energy applications, Sol. Energy Mater. Sol. Cell. 82 (2004) 491–515, https://doi.org/10.1016/j.solmat.2004.02.011.
[35] B. Ottersböck, G. Oreski, G. Pinter, How to accelerate natural weathering of polymeric photovoltaic backsheets – a comparison with standardized artificial aging, Sol. Energy Mater. Sol. Cell. 244 (2022) 111819, https://doi.org/10.1016/j.solmat.2022.111819.
[36] O. Raccurt, C. Delord, C. Bouquet, R. Couturier, Correlation between solar mirror degradation and colorimetric measurement of protective back layer, Energy Proc. 49 (2013) 1700–1707, https://doi.org/10.1016/j.egypro.2014.03.179.
[37] B. Suyitno, The assessment of reflector material durability for concentrated solar power based on environment exposure and accelerated aging test, E. Eur. J. Enterprise Technol. 6 (2022) 22–29, https://doi.org/10.15587/1729-4061.2022.265678.
[38] C. Avenel, O. Raccurt, J.-L. Gardette, S. Therias, Review of accelerated ageing test modelling and its application to solar mirrors, Sol. Energy Mater. Sol. Cell. 186 (2018) 29–41, https://doi.org/10.1016/j.solmat.2018.06.024.
[39] E. Schutz, F. Berger, R. Barillon, P. Audebert, A. Chambaudet, Behavior of painted mirrors during exposure tests of Salt spray, Appl. Surf. Sci. (1997).
[40] M. Zapponi, T. Pérez, C. Ramos, C. Saragovi, Prohesion and outdoors tests on corrosion products developed over painted galvanized steel sheets with and without Cr(VI) species, Corros. Sci. 47 (2005) 923–936, https://doi.org/10.1016/j.corsci.2004.06.007.
[41] EN ISO 9227:2022, Corrosion Tests in Artificial Atmospheres - Salt Spray Tests, 2022.
[42] F. Sutter, Y. Binyamin, T. Zoschke, A. Fernández-García, S. Naamane, M. Galetz, R. Reoyo-Prats, F.J. Pérez-Trujillo, A. Aglüro, F. Orioli, J. Piron, D. Mandler, A. Attout, S. Caron, J. Wette, R. Sánchez, A. Morales, C. Hildebrant, RAISELIFE project extends the lifetime of functional CSP materials, AIP Conf. Proc. 2445 (2022) 020013, https://doi.org/10.1063/5.0085763.
[43] A. Fernandez-Garcia, F. Sutter, M. Montecchi, F. Sallaberry, A. Heimath, C. Heras, E. Le Baron, A. Soum-Glaude, Parameters and method to evaluate the reflectance properties of reflector materials for concentrating solar power technology technology - official reflectance guideline version 3.1, SolarPACES (2020).
[44] ASTM E903-82, Standard Test Method for Solar Absorptance, Reflectance, and Transmittance of Materials Using Integrating Spheres, American Society for Testing and Materials, ASTM International, 1992.
[45] ASTM G173, Standard Tables for Reference Solar Spectral Lrradiances: Direct Normal and Hemispherical on 37° Tilted Surface, American Society forTesting and Materials, ASTM International, 2003 (n.d.).
[46] F. Buendía-Martinez, A. Fernandez-Garcia, F. Sutter, L. Martinez-Arcos, T.J. Reche-Navarro, A. Garcia-Segura, L. Valenzuela, Uncertainty study of reflectance measurements for concentrating solar reflectors, IEEE Trans. Instrum. Meas. 69 (2020) 7218–7232, https://doi.org/10.1109/TIM.2020.2975387.
[47] E. Schütz, F. Berger, O. Dirckx, A. Chambaudet, Study of degradation mechanisms of a paint coating during an artificial aging test, Polym. Degrad. Stabil. 65 (1999) 123–130, https://doi.org/10.1016/S0141-3910(98)00227-4.
[48] N. Voevodin, C. Jeffcoate, L. Simon, M. Khobaib, M. Donley, Characterization of pitting corrosion in bare and sol–gel coated aluminum 2024-T3 alloy, Surf. Coating. Technol. 140 (2001) 29–34, https://doi.org/10.1016/S0257-8972(01)01000-3.
[49] S. Bouaddi, A. Fernández-García, C. Sansom, J. Sarasua, F. Wolfertstetter, H. Bouzekri, F. Sutter, I. Azpitarte, A review of conventional and innovative-sustainable methods for cleaning reflectors in concentrating solar power plants, Sustainability 10 (2018) 3937, https://doi.org/10.3390/su10113937.
[50] A. García-Segura, A. Fernández-García, M.J. Ariza, F. Sutter, L. Valenzuela, Durability studies of solar reflectors: a review, Renew. Sustain. Energy Rev. 62 (2016) 453–467, https://doi.org/10.1016/j.rser.2016.04.060.
[51] J. Wette, F. Sutter, F. Buendía-Martínez, A. Fernández-García, Effect of long term outdoor exposure on anti-soiling coatings for solar reflectors, AIP Conf. Proc. 2303 (2020) 150016, https://doi.org/10.1063/5.0028960.
[52] Z.-S. Huang, C. Shen, L. Fan, X. Ye, X. Shi, H. Li, Y. Zhang, Y. Lai, Y.-Y. Quan, Experimental investigation of the anti-soiling performances of different wettability of transparent coatings: superhydrophilic, hydrophilic, hydrophobic and superhydrophobic coatings, Sol. Energy Mater. Sol. Cell. 225 (2021) 111053, https://doi.org/10.1016/j.solmat.2021.111053.
[53] F. Wiesinger, G. San Vicente, A. Fernández-García, F. Sutter, Á. Morales, R. Pitz-Paal, Sandstorm erosion testing of anti-reflective glass coatings for solar energy applications, Sol. Energy Mater. Sol. Cell. 179 (2018) 10–16, https://doi.org/10.1016/j.solmat.2018.02.018.
[54] M. Montecchi, F. Sutter, A. Fernández-Garćıa, A. Heimsath, F. Torres, C. Pelayo, Enhanced equivalent model algorithm for solar mirrors, AIP Conf. Proc. 2303 (2020) 100005, https://doi.org/10.1063/5.0028768.
[55] A. García-Segura, A. Fernández-García, M.J. Ariza, F. Sutter, L. Valenzuela, Degradation of concentrating solar thermal reflectors in acid rain atmospheres, Sol. Energy Mater. Sol. Cell. 186 (2018) 92–104, https://doi.org/10.1016/j.solmat.2018.06.032.
[56] L.F.E. Jacques, Accelerated and outdoor/natural exposure testing of coatings, Prog. Polym. Sci. 25 (2000) 1337–1362, https://doi.org/10.1016/S0079-6700(00)00030-7.
[57] F. Buendía-Martínez, F. Sutter, S. Gledhill, D. Argüelles-Arízcun, I. Cañadas, A. Fernández-García, Innovative lifetime testing protocol for high-temperature secondary reflector materials used in concentrated solar thermal energies, Sol. Energy Mater. Sol. Cell. 254 (2023) 112238, https://doi.org/10.1016/j.solmat.2023.112238.
[58] J. Wette, In-field analysis of microscopic degradation of solar reflectors. https://dgm.inventum.de/app/medialibrary/show/eventItem/57addb8e-d3c0-4f9f-9e43-5b02a775a57e, 2023.
[59] S. Lakhouil, S. Boukheir, A. Chbihi, S. Naamane, Outdoor exposure approach in a harsh environment toward the study of corrosion aspects of primary solar reflectors, Sol. Energy 230 (2021) 1070–1084, https://doi.org/10.1016/j.solener.2021.11.013.
[60] C.K. Ho, On-Sun Testing of a Heliostat Using Facets with Metallized Polymer Films, 2011, p. 8.